

Diffraction of non-uniformly polarized beams enables beam manipulation

Sai Nikhilesh Murty Kottapalli* and Alexander Song

Max Planck Institute for Intelligent Systems, Heisenbergstr. 3, 70569 Stuttgart, Germany

Peer Fischer†

Max Planck Institute for Intelligent Systems, Heisenbergstr. 3, 70569 Stuttgart, Germany and
Institute of Physical Chemistry, University of Stuttgart, Pfaffenwaldring 55, 70569 Stuttgart, Germany

The wave nature of light leads to interference and diffraction. A well known example of the wave nature is Thomas Young's double slit experiment, where light propagates through slits in an opaque screen to form a diffraction pattern at the detector. Here we extend this concept from opaque screens to spatially polarized wave fronts. The spatial variation of polarization gives rise to diffraction, opening the possibility to manipulate the beam shape and propagation direction via polarization control. We describe and simulate the propagation of a spatially inhomogeneous polarized wavefront and then experimentally demonstrate polarization control with a Bessel beam. Lensing in a beam without the need to change the phase-front of a beam is shown. We further explore how non-uniformly polarized beams may be used in combination with phase modulation for a high speed point scanning technique. This is in contrast to traditional methods of beam manipulation that make use of phase or amplitude modulation alone. Our work shows that diffraction due to polarization opens new possibilities for flexible and high speed beam control.

I. INTRODUCTION

Young's double slit experiment has long been used to demonstrate the wave nature of light. Coherent light passing through either of two adjacently placed slits interferes to produce a fringe pattern. The slits used in these experiments can be described as amplitude masks with maximal amplitude in the slits and zero everywhere else.

Here, we explore beams with non-uniform polarization structuring. We experimentally demonstrate and simulate a polarization analog of the famous double slit experiment and illustrate how interference of polarization can lead to the double-slit interference pattern. These patterns suggest how non-uniformly polarized wavefronts could enable applications in laser beam shaping and fast beam manipulation.

Laser beam shaping and manipulation plays an important role in many areas of science and technology such as microscopy and materials processing. Beam control and shaping has been achieved using lenses and mechanical deflectors and fine-grained dynamic control has been achieved by spatial modulation of phase and amplitude using devices such as spatial light modulators (SLM) and digital mirror devices (DMD) [5]. These optical components rely on spatial modulation of phase or amplitude, with a notable exception in the form of polarization singularities [4]. Here, we design polarization masks to implement particular optical functions. We experimentally demonstrate the generation of a Bessel beam profile from a Gaussian laser profile, which has applications in microscopy.

Fast dynamic control of beams has been of particular interest for many applications [7]. In this paper, we argue that a wavefront that utilizes variation in polarization, in combination with free-space diffraction, enables potentially fast and simple forms of beam control. We demonstrate how global rotation of a locally polarized wavefront can be used to quickly change a beam profile in time and when coupled with a static phase mask, allows for performing a high-speed scanning of a collection of points.

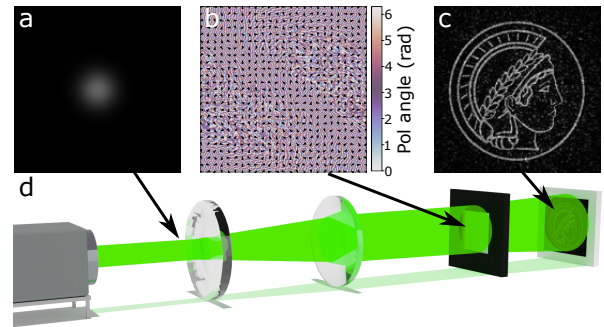


FIG. 1: Local control of the polarization orientation of a coherent beam can be flexibly controlled to generate intensity patterns. A Gaussian laser beam (a) propagates through an SLM where a pre-computed mask (b) is projected that locally rotates the polarization at each pixel. This mask is designed with a variant of the Gerchberg-Saxton algorithm (see Methods) to cause the beam to form an image of the Max-Planck Minerva (c) after a region of free-space diffraction. (d) depicts the optical setup.

Prior work on polarization beam control makes use of a global rotation of polarization to select between two orthogonal states [6] or displace the center of a beam [8]. These methods utilize polarization to dynamically control the laser beam but not for the purpose of shaping the beam. A second group of

* kottapalli@is.mpg.de

† fischer@is.mpg.de

techniques has used polarization for beam shaping, including the generation of vortex beams [4] and demonstration of a flat-top focusing [2] leading to interesting applications [1]. In these techniques, however, dynamic beam control has not been demonstrated.

Fig. 1 depicts the scheme that enables the generation of an image via polarization control and diffraction. A polarization mask is used to create a non-uniform polarization of the propagating coherent beam (Fig. 1c) without affecting the amplitude. The free-space propagation of the non-uniformly polarized wavefront gives rise to an image on a detector or screen.

II. METHODS

A. Experimental setup

A laser beam from a solid state CW laser source at 532nm (Oxxius Laser OXX-532-1000) is expanded to 5mm and the polarization is then rotated using a half-wave plate before the polarization of the propagating beam is locally rotated using a Holoeye LC2012 SLM at each pixel (1024×768) with a pre-calculated polarization mask. After further propagation for a pre-defined distance, the diffracted light is then imaged on a CMOS camera (Flir Oryx 10GiGE). A linear polarizer is placed before the camera in some experiments where a projection along a certain polarization orientation is necessary.

B. Simulation

The propagation of a wavefront of electromagnetic radiation with angular frequency ω in a homogeneous, isotropic, linear and source-free medium has to satisfy the vector Helmholtz equation:

$$(\nabla^2 + k^2)\mathbf{E}(\mathbf{r}) = 0 \quad (1)$$

where $k = (\omega/c)n$ and n is the refractive index. The field satisfying this equation can be written in the Fourier space

$$\mathbf{E}(x, y, z) = \frac{1}{2\pi} \iint_{-\infty}^{\infty} \hat{\mathbf{E}}(k_x, k_y; 0) e^{i[k_x x + k_y y \pm k_z z]} dk_x dk_y \quad (2)$$

This equation is called the *angular spectrum* representation of the electric field [3]. The propagation of any arbitrary field can be computed by solving this integral using FFTs on a computer. The evolution of the two orthogonal polarization states, $\mathbf{E}_x(x, y, z)$ and $\mathbf{E}_y(x, y, z)$, can be independently computed. We then use the Jones matrix formalism to calculate the resultant field after propagation.

The initial field \mathbf{E}_0 , polarized along the orientation of the liquid crystal, is discretized to correspond to the smallest pixel size of the spatial light modulator used in the experiment. The polarization of the initial field is rotated by an angle α dependent on the voltage applied at each pixel. The field is then split into two orthogonal components of the polarization, E_x and E_y as follows

$$\begin{bmatrix} E_x \\ E_y \end{bmatrix} = \begin{bmatrix} E_0 \cos \alpha \\ E_0 \sin \alpha \end{bmatrix} \quad (3)$$

The two orthogonally polarized components, \mathbf{E}_x and \mathbf{E}_y , of the incident field are then treated separately by performing two independent angular spectrum calculations. An analyzer can also be simulated using Jones calculus. The calculations are performed pixel-wise over the entire field at any given plane. The intensity of the obtained diffraction pattern is then compared with the experimental results.

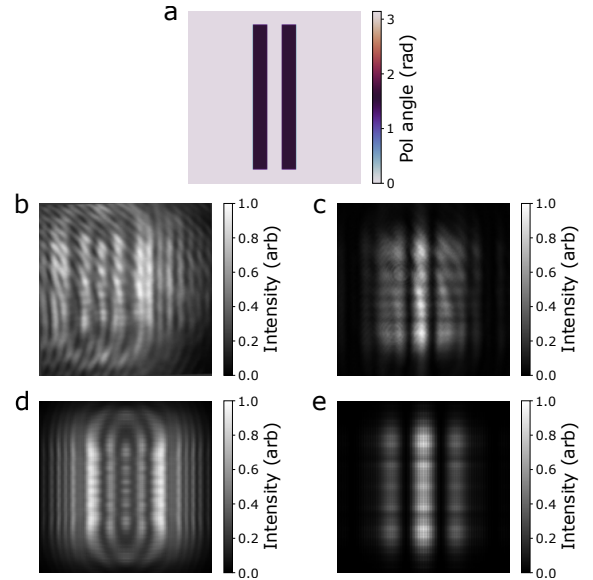


FIG. 2: A Young's double slit analog in the polarization domain. A polarization mask consisting of two stripes (a) is placed in the path of a Gaussian laser beam with a polarization rotation of $\pi/2$ radians within the stripes and zero everywhere else. The experimentally obtained results for a 500 mm propagation without (b) and with the analyzer (c). The corresponding simulated propagation outputs without (d) and with (e) an analyzer show the same spatial modulation.

To calculate a polarization mask that generates a desired wavefront amplitude after a certain propagation distance (Figure 1, the Gerchberg-Saxton phase retrieval algorithm [9] is modified to use free-space propagation from the simulation above. A phase mask is estimated using the procedure with a desired input-output image pair. This mask is converted to the angle of polarization rotation used in the above simulator and propagated forward, serving as a coarse polarization analog of the calculated phase mask.

III. RESULTS AND DISCUSSION

A. Young's double slit analog

To understand the effect of spatially structuring polarization on the propagating wavefront, we consider the example of a Young's double slit analog as shown in Fig. 2. Instead of an amplitude or phase mask, a polarization image with two vertical stripes, each corresponding to a $\pi/2$ radians polarization rotation (Fig. 2a) is uploaded and presented on the SLM. Crucially, the intensity remains unchanged in this example. As the light propagates, diffraction ensues before the light beam is imaged onto a camera. The detected pattern (Fig. 2b) can be understood as the summation of the diffraction pattern of the two complementary orthogonally polarized fields. When an analyzer is placed in front of the camera, one of the two diffraction patterns can be selected, as shown in Fig. 2c for an analyzer oriented along $\pi/2$ radians.

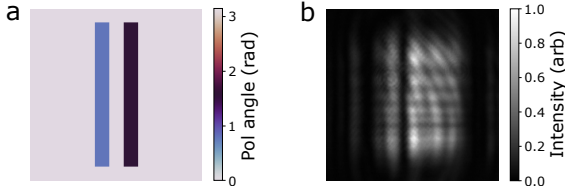


FIG. 3: A Young's double slit analog in the polarization domain when each of the slit-analogs corresponds to different polarization rotations. The input, as shown in (a), consists of two stripes that rotate the polarization of the propagating beam by unequal amounts, $\pi/4$ and $\pi/2$ respectively. The output in the experiment (b) is then captured on a camera after a propagation of 500mm.

To rule out the contribution from the added geometric phase from the SLM during a polarization rotation operation, we simulated the propagation of polarized light with similar conditions to that in the experiments using the method described in Sec. II B. The obtained diffraction patterns with and without an analyzer, as can be seen in Fig. 2d and Fig. 2e respectively, show qualitatively similar structure to the experimentally obtained results while only accounting for inhomogeneous polarization. This shows that strong perturbations to the beam profile can be achieved with spatial structuring of polarization. These effects are not restricted to only orthogonally polarized beam contributions, but also appear during diffraction of the beam with intermediate polarization levels across the wavefront (Fig. 3), which may be used to form more complex beam profiles.

B. Bessel beam shaping

Our experiments demonstrate that diffraction of a uniform beam is affected by the polarization across the wavefront. We explore how this can be utilized for beam shaping by generating a Bessel beam. Bessel beams are typically generated by introducing a linearly increasing radial phase e.g. with an axicon or a phase-only SLM. Using a polarization rotation mask has, to the best of our knowledge, not been used previously as a means to achieve focusing. In this experiment, a Bessel mask rotates the polarization of the propagating wavefront between 0 radians and $\pi/2$ radians, as shown in Fig. 4a. The beam is then allowed to propagate for 500mm and is imaged on a camera, with an analyzer (Fig. 4a) and without an analyzer Fig. 4c in between. We observe a 2D Bessel function as can be seen in both cases, which suggests that each independent linear polarization state can implement the Bessel-forming function.

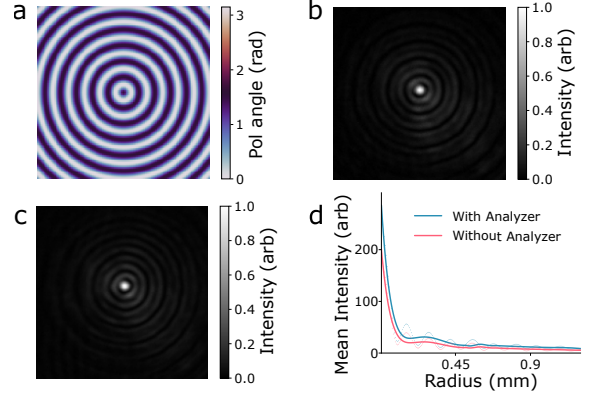


FIG. 4: Experimental results for Bessel beam shaping via polarization modulation. (a) The polarization mask that leads to the output pattern with (b) and without (c) an analyzer captured on the detector. (d) A comparison between radial averages from the center of the focal point shows the Bessel function shape.

C. Dynamic Control

Using polarization masks to obtain desired diffraction patterns offers the possibility of fast dynamic control of laser light. Fast spatial scanning is of great interest in microscopy and typically mechanical devices like galvanometers or MEMS micro-mirrors are used for these applications. However, scanning can also be performed instead by rotating the polarization, for instance, with a Pockels cell while avoiding the drawbacks of using fast-moving mechanical parts. As a demonstration of a possible implementation, we demonstrate a technique can for scanning five spatially separated points on the image plane.

The setup used for performing these experiments is seen in Fig. 5a. A phase mask (Fig. 5c or d) is projected onto the phase SLM (R-SLM), corresponding to a diffraction pattern (Fig. 6a or b). A sinusoidally varying polarization mask (Fig. 5b, T-SLM) is then applied onto this wavefront. An analyzer selects for the desired points displayed on the image plane.

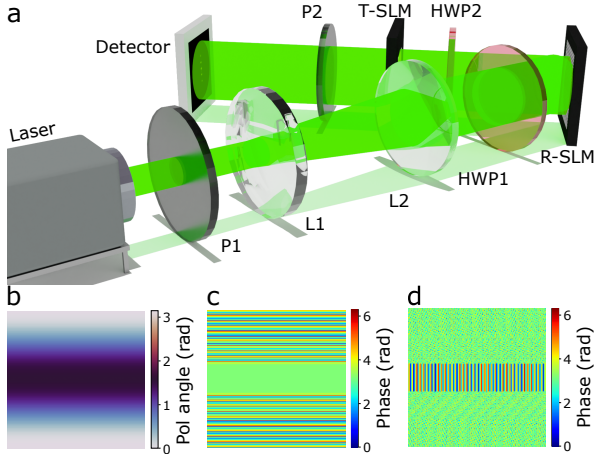


FIG. 5: (a) Experimental setup used for performing scanning of multiple points. A 532nm laser beam is polarized using the polarizer P1 and is then expanded using the lenses L1 and L2 and half wave plates HWP1 and HWP2 ensure the correct polarization for the phase and polarization SLMs, R-SLM and T-SLM respectively. An analyzer P2 then selects the desired polarization state. (b), (c) and (d) polarization mask, phase masks corresponding to the straight line projection, and for projecting a set of arbitrary points, respectively.

Fast scanning rates can be achieved by rotating the polarization at a high modulation rate using an electrooptic modulator such as a Pockels cell which automatically results in fast beam deflection and hence scanning rates. The nature of the diffraction pattern can also be changed by tuning the computer generated phase masks. In our experiments, we have demonstrated the two cases where the five points are distributed in a straight line and where the five points are distributed arbitrarily. The phase masks used to achieve these patterns can be seen in Fig. 5c and Fig. 5d, respectively.

We explore the relation between the intensities of these five independent points by examining the intensity evolution in a square box of dimension $86\mu\text{m} \times 86\mu\text{m}$ centered at the points. As can be seen from Fig. 6c and 6d, the intensity evolution shows a sinusoidal behavior but the maximum intensity in these points is reached at different times. This is also seen in Fig. 6e and Fig. 6f. This technique can be used to perform high speed point scanning along arbitrary points with a stationary phase and polarization mask and only an electrooptic modulator as a dynamic component, replacing

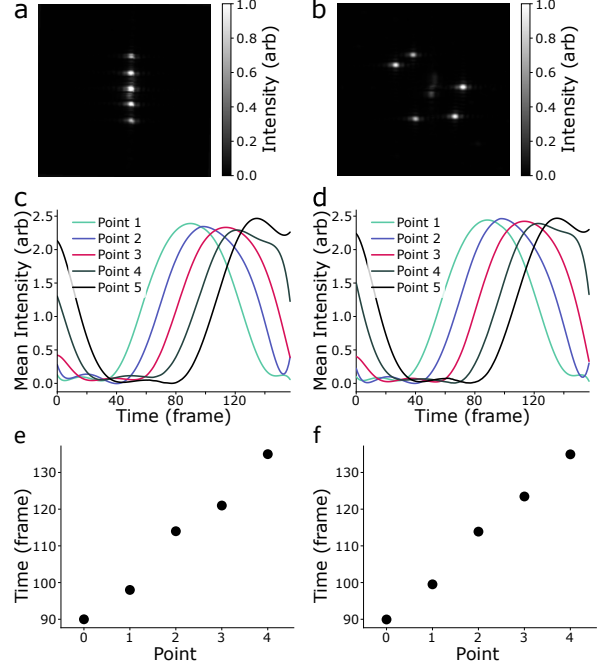


FIG. 6: Point scanning with global polarization rotation. (a), (b) the projected points corresponding to the two phase masks shown in Fig. 5(c), (d) respectively. (c), (d) evolution of the intensity in the projected points for the straight line and arbitrary case. (e), (f) compilation of the time it takes to attain maximum intensity for each of the points.

the need for moving mechanical parts and large scanning optics.

IV. CONCLUSION

In the current work we show that a variation of polarization across a beam front with constant amplitude and phase can also give rise to diffraction. We explore how the combination of free-space propagation with continuous polarization masks may be used to perform certain beam-shaping and displacement operations. We describe a model of these operations using an analog of the Young's double slit as an example and experimentally validate the results. A potentially useful application of this system can perform a beam transformation of a Gaussian beam into a Bessel beam. As this technique is complementary to other beam control techniques, we demonstrate a proof-of-concept polarization-based point scanning system that relies on global rotation of a wavefront polarization. These ideas pave the way for the future development of non-mechanical scanning systems with extremely high speeds. More generally, we expect this work to inspire the development of novel optical imaging and fabrication methods where sophisticated manipulation of polarization enables better control of laser beams.

ACKNOWLEDGMENTS

The authors thank the International Max Planck Research School for Intelligent Systems (IMPRS-IS) for supporting Sai Nikhilesh Murty Kottapalli.

-
- [1] Thomas G Brown and Amber M Beckley. Stress engineering and the applications of inhomogeneously polarized optical fields. *Frontiers of Optoelectronics*, 6(1):89–96, 2013.
 - [2] Hao Chen, Santosh Tripathi, and Kimani C Toussaint. Demonstration of flat-top focusing under radial polarization illumination. *Optics letters*, 39(4):834–837, 2014.
 - [3] PJB Clarricoats. The plane wave spectrum representation of electromagnetic fields. *Electronics and Power*, 13(5):176, 1967.
 - [4] Mark R Dennis, Kevin O’Holleran, and Miles J Padgett. Singular optics: optical vortices and polarization singularities. *Progress in optics*, 53:293–363, 2009.
 - [5] Fred M Dickey, Scott C Holswade, et al. *Laser beam shaping*. Marcel Dekker New York, 2000.
 - [6] Markus Fratz, Dominik M Giel, and Peer Fischer. Digital polarization holograms with defined magnitude and orientation of each pixel’s birefringence. *Optics letters*, 34(8):1270–1272, 2009.
 - [7] SeungYeon Kang, Martí Duocastella, and Craig B Arnold. Variable optical elements for fast focus control. *Nature Photonics*, 14(9):533–542, 2020.
 - [8] Luis José Salazar-Serrano, David A Guzmán, Alejandra Valencia, and Juan P Torres. Demonstration of a highly-sensitive tunable beam displacer with no use of beam deflection based on the concept of weak value amplification. *Optics express*, 23(8):10097–10102, 2015.
 - [9] Guo-zhen Yang, Bi-zhen Dong, Ben-yuan Gu, Jie-yao Zhuang, and Okan K Ersoy. Gerchberg–saxton and yang–gu algorithms for phase retrieval in a nonunitary transform system: a comparison. *Applied optics*, 33(2):209–218, 1994.